

# Dual-Mode PSK Transceiver on SDR With FPGA

Wuqiong Zhao<sup>✉</sup>, *Student Member, IEEE*

(This is a draft version and has not been fully edited.)

**Abstract**—In this experiment, we implement a dual-mode PSK transceiver on SDR with FPGA, supporting both BPSK and QPSK. Moreover, the transceiver is designed to be able to switch between the two modes by introducing a packet-based communication protocol, where modulation information can be extracted from the packet header. Both simulation results and experiment observations on an SDR platform verify the effectiveness of the design.

**Index Terms**—Phase-shift keying (PSK), software-defined radio (SDR), transceiver design, modulation, demodulation, field programmable gate array (FPGA).

## I. INTRODUCTION

SOFTWARE-DEFINED radio (SDR) is useful in various applications, including rapid prototyping and research. A millimeter wave (mmWave) SDR platform [1] can enable research in both mmWave physical-layer communications and the high-level networking problems.

Phase-shift keying (PSK) is a popular modulation scheme in digital communications, the simplest two schemes are the binary PSK (BPSK) and the quadrature PSK (QPSK). The carrier extraction is required for coherent demodulation, though differential encoding can be used to avoid the carrier extraction.

Field programmable gate array (FPGA) is a popular choice for SDR baseband processing, due to its flexibility and high performance. In this project, instead of employing high-level synthesis (HLS) [2], we directly implement the transceiver on FPGA using hardware description language (HDL) Verilog, for a better control of the underlying hardware, and reduce the resource consumption.

To benefit the research and learning community, the design sources (Vivado project) and this paper (in L<sup>A</sup>T<sub>E</sub>X) are open source [3].

The contributions of this paper is summarized as follows:

- 1) We implement a dual-mode PSK transceiver on SDR with FPGA, enabling both BPSK/QPSK modulation and demodulation, with carrier synchronization and symbol synchronization.
- 2) A packet-based communication is introduced to enable the switching between BPSK and QPSK based on header

fields, another step towards to a flexible and ready-to-use transceiver.

- 3) The open-source design is implemented on a Zynq-7020 FPGA and verified on an SDR platform, demonstrating its effectiveness.

## II. SYSTEM OVERVIEW

### A. Software-Defined Radio

We employ eNodeX [4], an SDR platform equipped with a pair of configurable Global System for Mobile Communications (GSM) transmitter (Tx) and receiver (Rx) antennas.

### B. Transceiver Design

The current transmitter and receiver are implemented on the same FPGA, but can be readily extended to different FPGAs with small frequency offsets. The system overview is shown in Fig. 1.

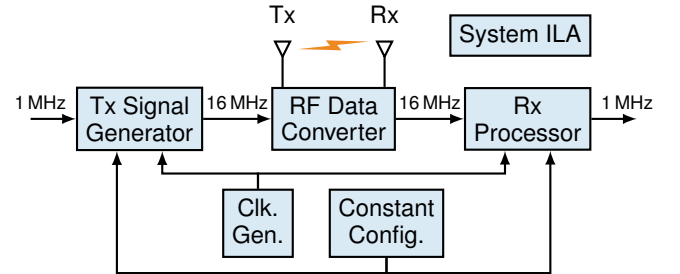


Fig. 1. Transceiver system overview.

**Clock Generator.** Required clocks are generated from the PL clock. All reset signals are generated using Processor System Reset Modules [5], which can provide synchronized power-up reset signals.

**RF Data Converter.** This block contains analog-to-digital converter (ADC) and digital-to-analog converter (DAC), enabled by a vendored AD9361 module.

**Tx Signal Generator.** The transmitted signal is generated in this block. Currently, it repeats a certain pattern and does not accept external input. But it can be readily extended to a more complicated design, based on the current interface template.

**Rx Processor.** This block is responsible to process the received signal, including demodulation and data extraction from a packet. It is the most complicated block in the system.

**System ILA.** The system integrated logic analyzer (system ILA) [6] is used to observe the internal signals.

**Constant Configurations.** Several parameters can be configured in this block. Most importantly, the mode control constants (MODE\_CTRL) are shown in Table I.

Date of publication 10 January 2024; date of current version 10 January 2024. The author would like to thank Lecturer Dan Yang for the guidance and help in the course of the experiment. The author would also like to thank AI tools including GitHub Copilot and Claude.AI for their help in preparing this paper.

Wuqiong Zhao is with Southeast University, Nanjing 211189, China. (e-mail: wqzhao@seu.edu.cn, website: <https://wqzhao.org>).

Online URL: <https://go.wqzhao.org/sdr-psk-fpga>

TABLE I  
MODE CONTROL CONSTANTS

Mode	Localparam	Value	is_bpsk	Packet
BPSK	MODE_BPSK	4'b0001 (1)	1'b1	No
QPSK	MODE_QPSK	4'b0010 (2)	1'b0	No
Mixed	MODE_MIX	4'b0100 (4)	variable	Yes

As shown in Table I, the system can be configured to work in BPSK, QPSK, or the mixed mode. The remaining part will focus on the mixed mode, which has MODE\_CTRL equal to MODE\_MIX (4'b0100).

### C. BPSK/QPSK Modulation

The BPSK and QPSK modulation constellation graphs used in our system are shown in Fig. 2. Different from the traditional setting, our adopted BPSK constellation in Fig. 2(a) is a combination of in-phase (I) and quadrature (Q) components. This is to make sure the phases used in BPSK are among those in QPSK, to ensure a smooth transition between the two modes, especially because the header field is always modulated in BPSK.

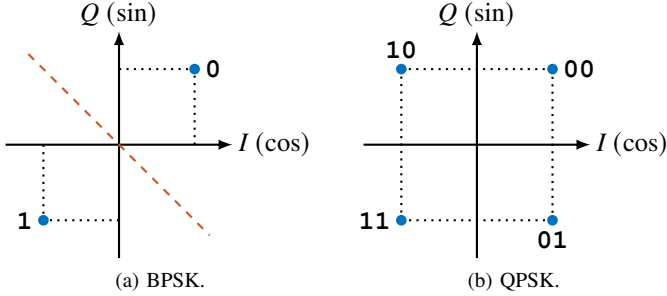


Fig. 2. BPSK/QPSK modulation constellation used in our system.

## III. TRANSMITTER

### A. Carrier NCO

The carrier frequency is generated by a numerically controlled oscillator (NCO). In Vivado, we use the Direct Digital Synthesis (DDS) Compiler IP [7] to generate the NCO. Both the cosine and sine components are used.

### B. PSK Modulation

1) *Pseudo-random Noise (PN) Generator*: In this experiment, the transmitted signal are pseudo-random noise (PN) sequences. Typically, we implement the PN generator with  $N = 4$  and  $N = 5$  with a shift register [8]. The Verilog code for the module PN\_Gen is shown below.

```

module PN_Gen # (parameter N = 5) (
    input    clk,
    output reg pn
);
    reg [N-1:0] PN_buf = 1; wire rst;
    generate
    if (N == 5)
        always @ (posedge clk)
            if (rst) begin PN_buf <= 5'd1; pn <= 0; end
    endgenerate
endmodule

```

```

else begin
    PN_buf <= { PN_buf[3:0], PN_buf[4] ^ PN_buf[2] };
    pn <= PN_buf[4];
end
else if (N == 4)
    always @ (posedge clk)
        if (rst) begin PN_buf <= 4'd1; pn <= 0; end
    else begin
        PN_buf <= { PN_buf[2:0], PN_buf[3] + PN_buf[2] };
        pn <= PN_buf[3];
    end
else ; // NOT implemented yet!
endgenerate
assign rst = !(|PN_buf); // reset when PN_buf is all 0
endmodule

```

2) *Modulation With I and Q Streams*: The modulation is performed by multiplying selecting the appropriate carrier phase according to the input bits and the constellation. Note the Q component always has a phase  $90^\circ$  ahead of the I component.

## IV. RECEIVER

### A. Overview

The receiver performs carrier synchronization, symbol synchronization and PSK detection first, without considering the packet structure. The depacketizer and the packet extraction is based on the synchronized bit stream after PSK detection.

### B. Carrier Synchronization Using Costas Loop

A Costas loop [9] is used for carrier synchronization. The basic idea of a Costas loop is to provide an error (carrier phase offset) feedback. The negative feedback is used to lock the carrier phase to the PSK signal. The generation of the error feedback is specific to different modulation schemes, as well as their constellation graphs.

The proposed dual-mode Costas loop is shown in Fig. 3, which can be switched between BPSK and QPSK via a control signal *is\_bpsk*. The two multipliers directly following the PSK stream input are phase detectors, whose low-frequency components represent the baseband signal. Therefore, the baseband I and Q signal can be extracted after passing through a low-pass filter (LPF). Thus, it is ready to map the obtained I/Q signal to the constellation graph, and generate the error signal when comparing with the designed one.

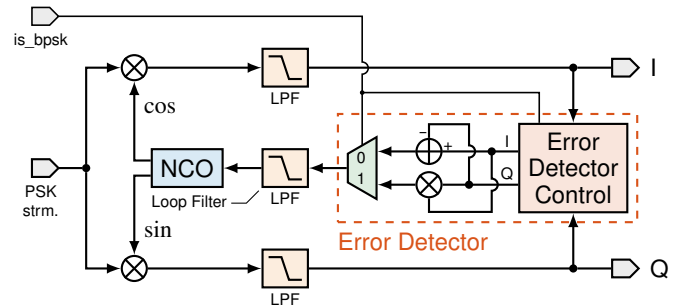


Fig. 3. Costas loop for carrier synchronization with BPSK/QPSK support.

The error feedback for BPSK is defined as

$$e_{\text{BPSK}} = (I + Q) \times (I - Q), \quad (1)$$

and the error feedback for QPSK is defined as

$$e_{\text{QPSK}} = I \cdot \text{sgn}(Q) - Q \cdot \text{sgn}(I). \quad (2)$$

For stability, the loop filter as an LPF is added before the error is fed back to the NCO. The NCO implemented with DDS has the phase defined as

$$\begin{aligned} \phi[n] &= \phi[n-1] + \Delta\phi[n] \\ &= \phi[n-1] + (f_0 + k \cdot f_{\text{feedback}}), \end{aligned} \quad (3)$$

where  $\phi[n]$  is the phase increment at time  $n$ ,  $f_0$  is the free running clock (4.096 MHz in our design), and  $k$  is the feedback coefficient. The core Verilog implementation of the Error Detector Control is given below, which shows that for QPSK, the feedback value is arithmetically right shifted by 6 bits to match the scale of that in BPSK.

```

if (is_bpsk) begin // BPSK
    out_I_tdata <= in_I_tvalid ? in_I_tdata + in_Q_tdata : 0;
    out_Q_tdata <= in_Q_tvalid ? in_I_tdata - in_Q_tdata : 0;
end
else begin // QPSK
    out_I_tdata <= in_I_tvalid ? (in_Q_tdata[WIDTH-1] ?
        -in_I_tdata : in_I_tdata) >>> 6 : 0;
    out_Q_tdata <= in_Q_tvalid ? (in_I_tdata[WIDTH-1] ?
        -in_Q_tdata : in_Q_tdata) >>> 6 : 0;
end

```

In the Costas loop, the feedback coefficient  $k$  is an important coefficient to finetune according to the system. This parameter is reflected as `FEEDBACK_SHIFT`, and  $k \triangleq 2^{-\text{FEEDBACK\_SHIFT}}$ . The convergence of the Costas loop under different carrier frequency offset (CFO) is discussed in Section VI-B.

### C. Symbol Synchronization Using Gardner Loop

A Gardner loop [10] is used to achieve symbol (timing) synchronization. The structure of a Gardner loop is shown in Fig. 4. The loop itself is not directly shown in the figure,

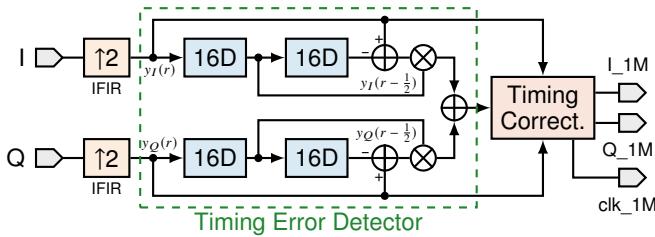


Fig. 4. Structure of a Gardner loop for symbol timing synchronization.

To reduce implementation complexity, we use the sign of strobe values as mentioned in [10]. The total symbol timing error considering I and Q components is

$$\begin{aligned} u_t(r) &= y_I(r - \frac{1}{2}) [\text{sgn}(y_I(r)) - \text{sgn}(y_I(r-1))] \\ &\quad + y_Q(r - \frac{1}{2}) [\text{sgn}(y_Q(r)) - \text{sgn}(y_Q(r-1))], \end{aligned} \quad (4)$$

where  $r$  has a symbol frequency of 1.024 MHz. For better timing performance, we linearly interpolate the 16.385 MHz input I/Q data to 32.768 MHz. Therefore,  $y_I(r-1)$  and  $y_Q(r-1)$  are delayed by 32 clocks. In FPGA implementation, for each I/Q stream, two shift registers of depth 16 are used. Notably, since we adopt the BPSK constellation in Fig. 2(a),

the symbol timing error depends on both I and Q components, the same as QPSK. The correctness of symbol timing is shown in Fig. 10.

### D. PSK Detection

The detection is based on the constellation graph in Fig. 2, and the I/Q signals after the symbol synchronization.

## V. PACKET-BASED COMMUNICATION

### A. Frame Structure

The frame structure is shown in Fig. 5, consisting of the TRN, HDR and the PLD fields.

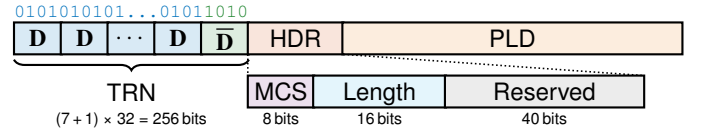


Fig. 5. Frame structure of the packet-based communication.

**Training (TRN).** The training field is used to provide packet timing information (coarse synchronization), as well as synchronize the carrier and symbol timing. It consists of 7 repetitions of  $\mathbf{D}$  and one  $\bar{\mathbf{D}}$ , where  $\mathbf{D}$  and  $\bar{\mathbf{D}}$  are of length 32.  $\mathbf{D}$  and  $\bar{\mathbf{D}}$  are repetitive sequences of '01' and '10', respectively. The training field from bit 0 to  $(7+1) \times 32 - 1 = 255$  is defined as

$$\text{TRN}[i] = \begin{cases} \text{mod}(i, 2), & i = 0, 1, \dots, 223, \\ \text{mod}(i + 1, 2), & i = 224, 225, \dots, 255. \end{cases} \quad (5)$$

Notably, the phase transition from bit 223 to 224 is used to indicate the boundary of the packet.

**Header (HDR).** The header field is used to provide packet information, including the modulation and coding scheme (MCS) and the packet length (Length) in bits. The remaining bits are reserved for future use. The MCS field currently only determines the use of BPSK or QPSK. The MCSs for BPSK and QPSK are defined as '01010101' and '10101010' respectively.

**Payload (PLD).** The payload field is used to carry the actual data. Its length in bits (1 bit for each BPSK symbol, 2 bits for each QPSK symbol) should match the Length field in the header.

### B. Packetizer Design

The packetizer FSM has 5 states: IDLE, HDR, PLD, LAST and WAIT. The IDLE state is used to wait for the packet start. It transits to the HDR state when the valid and ready signals are both high, i.e., the packet starts transmitting. The HDR state is used to transmit the header (including TRN and HDR)<sup>1</sup>, as discussed in Section V-A. It then transmits to the PLD state<sup>2</sup> to transmit the payload stored in the FIFO. Notably, the FIFO depth should not be smaller than the header

<sup>1</sup>For the packetizer, we do not distinguish TRN and HDR for simplicity, and they are called the header in contrast to the payload.

<sup>2</sup>If the payload symbol length is 1, it will directly transit to the LAST state.

length (i.e. 320). The LAST state is used to transmit the last symbol of the payload, when the `AXIS_tlast` signal will be high. After transmitting all payload data, the WAIT status is employed to consume all remaining data in the FIFO. This is only used in our design to better demonstrate the relationship between the transmitted bits and the received bits, and this status can be removed for other applications. Finally, after the FIFO is cleared, the state will transition to the IDLE state waiting for new data income.

### C. SPB Detection

SPD detection consists of strength detection (SD), packet detection (PD) and boundary detection (BD). They jointly provide information for the coarse packet timing.

1) *Strength Detection (SD)*: The strength detection checks the baseband I/Q amplitude from the Costas loop. It is useful because the PSK detector will always output a value, and it can confuse the packet parsing when the noise coincides with the packet sequence. For stability, the `SD_flag` is asserted when either the I or Q signal amplitude is larger than `RX_SD_THRESHOLD` at one clock within the window of `RX_SD_WINDOW` clocks.

2) *Packet Detection (PD)*: The presence of a packet can be identified by detecting repetitive ‘010101...’ sequence (modulated using BPSK). This can be performed by checking the continuous 1s for the differential results. The `PD_flag` is asserted when the differential results remain 1 for `RX_PD_WINDOW` clocks. Interestingly, the packet detection itself does not require a synchronized carrier, as a carrier phase shift does not significantly affect the ‘01’ sequence detection.

3) *Boundary Detection (BD)*: Exploiting the phase transition from bit 223 to 224 in the training field (see Section V-A and Fig. 5), the boundary detection can be performed by checking the differential value being 0 after the `PD_flag` being asserted. To ensure stability, the `BD_flag` is asserted after `RX_BD_WINDOW` clocks of continuous 1s in differential values. At boundary detection, the sign of the bit 223 and 224 are also recorded in `BD_sgn`, which can be used to counter the phase ambiguity in BPSK demodulation.

### D. Depacketizer Design

The depacketizer works the opposite way of the packetizer. It has 6 states: IDLE, TRN, HDR, PLD, LAST and WAIT. The TRN and the HDR state must be distinguished because the need to extract useful information in the TRN field. The IDLE state transits to the TRN state when `BD_flag` is high. Since the `BD_flag` contains the packet timing information, the depacketizer can count the number of clocks to determine the start of the HDR field. In the HDR field, both the MCS and packet length are extracted. Then, the depacketizer transits to the PLD state to extract the payload. The `tuser` signal is used to indicate the modulation scheme (1 for BPSK and 0 for QPSK). The `tlast` signal is used to indicate the end of the payload, at the LAST state. To correct disassert the PD and BD signal, the WAIT state is employed to wait for one more clock before it comes to the IDLE state.

## VI. SIMULATION RESULTS

In all Verilog simulation, random noise is added to the Rx ADC, to better simulate the real-world scenario.

### A. Transmitter

The transmitter DAC simulation results are shown in Fig. 6.

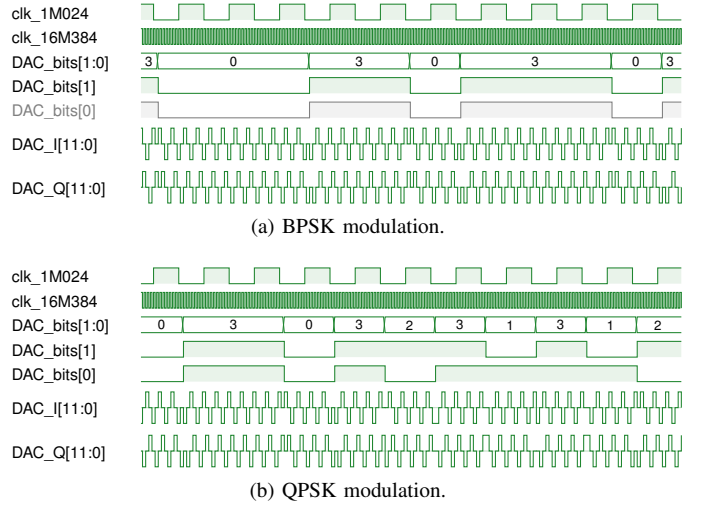


Fig. 6. DAC simulation results of the transmitter.

Due to the limited number of samples (4 per period), the DAC output is not smooth, and shapes like a triangle wave. Nevertheless, the phase shift for both I and Q at symbol transitions is clear.

### B. Carrier Synchronization Convergence

The simulation results of the Costas loop are shown in Fig. 7. In the BPSK mode, the Costas loop can successfully handle the CFO smaller than 7.81 kHz. It can be verified by the fact that the feedback saturates around a constant (corresponding to the CFO value), which . In the QPSK mode, the value is 1.96 kHz. The convergence is relatively fast.

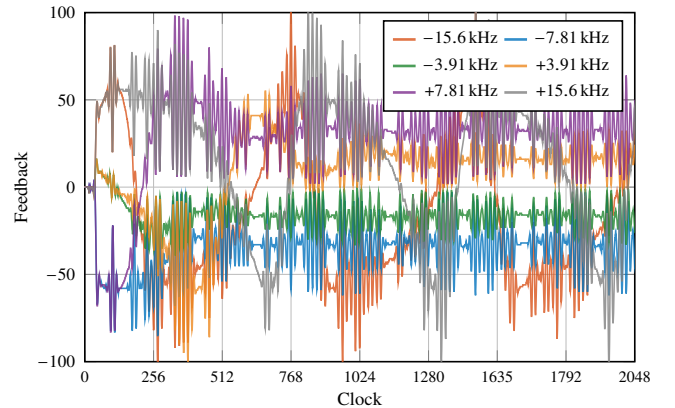


Fig. 7. Carrier synchronization for BPSK. The feedback value after the loop filter v.s. time, with different CFO.

Notably, the convergence performance of QPSK is poorer than BPSK in the current parameter set, which is by design.



For a dual-mode system which transmits payload in both BPSK and QPSK with a BPSK header, so the carrier synchronization is achieved at the BPSK header, therefore, QPSK does not need a strong feedback. Furthermore, the smaller feedback makes the BPSK and QPSK transmission smoother, avoiding a sudden phase jump of  $90^\circ$ .

### C. Mixed-Mode Receiver

In this simulation, we show the successful transmission of packets in both BPSK and QPSK modulations. The simulation results are shown in Fig. 8.

The two packets are clearly shown, with the first being QPSK and the second being BPSK, both of 128 bits length. The `Rx_tuser` signal shows the detected modulation scheme at the Rx, with 1 for BPSK and 0 for QPSK. Since QPSK has a  $2\times$  bit rate, the first packet payload is transmitted  $2\times$  faster than the first one.

## VII. FPGA IMPLEMENTATION

The design is implemented in Vivado 2022.2 using block diagrams. Some block diagram designs are shown in Section A.

The hardware resources consumption on Zynq-7020 (xc7z020clg484-1) with the default synthesis and implementation strategy is shown in Table II. Therefore, the design itself is area-efficient, and can be readily incorporated into a larger system.

TABLE II  
HARDWARE RESOURCES CONSUMPTION ON ZYNQ-7020

Resource	Utilization	Available	Util. Rate
LUT	7,248	53,200	8.04%
LUTRAM	1,121	17,400	6.44%
FF	8,144	106,400	7.65%
BRAM	27	140	19.29%
DSP	51	220	23.18%
IO	33	200	16.50%
BUFG	10	32	31.25%
MMCM	2	4	50.00%

## VIII. EXPERIMENT RESULTS ON SDR

The eNodeX SDR platform is configured to provide 1 Tx and 1 Rx at a sampling frequency of 16.384 MHz. The GSM antenna carrier frequency is 800 MHz, and the two antennas have a line-of-sight (LoS) channel.

The experiment results are observed via a system ILA in Vivado, and 4 general-purpose input/output (GPIO) pins are used to output some 1-bit signals, including the 1-bit Tx and Rx data stream and their corresponding clock.

In our design, 4 GPIO pins are connected, as listed in Table III. Fig. 9 shows the oscilloscope results of the GPIO outputs.

Fig. 9(a) and Fig. 9(b) connects the `GPIO_TH1` and `GPIO_TH2` pins, showing the transmitted 1-bit sequence (Tx) and the respective received 1-bit sequence (Rx). Clearly, the sequence is successfully recovered in both cases, with a certain time delay. The structure of `pn_5` sequence in BPSK is clearly

TABLE III  
GPIO PIN CONNECTIONS

Pin	Signal
GPIO_TH1	Tx 1-bit sequence (clock: 1.024 MHz or 2.048 MHz)
GPIO_TH2	Rx 1-bit sequence (sync. w/ Rx timing clock when BPSK)
GPIO_TH3	2.048 MHz global clock from the clock divider
GPIO_TH4	Rx timing clock ( $\sim 1.024$ MHz)

seen in Fig. 9(a), which has a bit frequency of 1.024 MHz. By contrast, the bit frequency of QPSK packets in Fig. 9(b) is 2.048 MHz. The symbol timing clock is shown in Fig. 9(c), which is not synchronized with the Rx data in BPSK, as the Rx data is connected after a FIFO with the master clock of 1.024 MHz.

Fig. 10 gives the ILA results for two cases involving BPSK and QPSK. The ILA results are consistent with the oscilloscope results, and provide additional insight into the system, including PSK detection and packet extraction. The `I_16M` and the `Q_16M` signals are the I and Q components of the baseband signal from the Costas loop, while the `I_1M` and the `Q_1M` signals are provided by the Gardner loop after symbol timing. The `out_clk_1M` clock is the symbol timing clock, which is near optimal, as designed by the Gardner loop.

## IX. DISCUSSIONS

### A. Possible Enhancement

**Frame structure design.** CRC and/or checksums can be added to the frame structure to enhance the packet transmission stability.

**Changing parameters on the fly.** AXI peripheral [11] can be used to change the parameters in the `Constant_Config` on the fly, if the board allows.

### B. Possible Extensions Beyond the Experiment

The training (TRN) field can be better utilized for additional experiments. For example, signal-to-noise (SNR) can be estimated at the TRN field. Channel estimation algorithms [12], [13] can also be investigated on the platform. It is also possible to investigate the auto generation [14] of digital circuits.

## X. CONCLUSION

In this paper, we implement the PSK transceiver with modulation and demodulation on FPGA. It successfully demonstrates the high-level system design, and communication techniques such as carrier synchronization, symbol synchronization and packet-based communication.

## APPENDIX A BLOCK DIAGRAMS

### A. Block Diagrams Design

The top level block diagram corresponding to Fig. 1 is shown in Fig. 11, and the Rx processor block diagram is shown in Fig. 12. Among the Rx processor, the Costas loop and the Gardner are both inserted block diagrams.



Fig. 8. Mixed-mode simulation results.

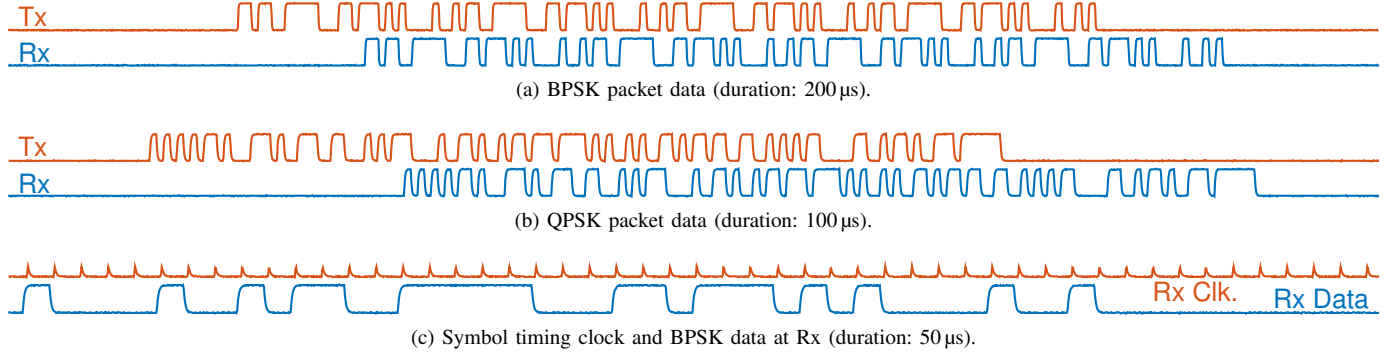


Fig. 9. Two-channel oscilloscope results of GPIO outputs.

The Costas loop is shown in Fig. 13, where the phase detectors are implemented using the multiplier IP [15], and the NCO hierarchy is mainly composed of the DDS Compiler IP [7].

More block diagrams are provided at <https://github.com/Teddy-van-Jerry/sdr-psk-fpga/tree/master/schematic> [3].

### B. Debugging With Block Diagrams

**AXI connections.** AXI and AXI stream (AXIS) interfaces should be carefully dealt with in the block diagram. When connecting one of the signal in the bus elsewhere (e.g., to ILA), a manual connection of the signal to the corresponding AXIS interface signal is required. Besides, when the AXI interface is not associated with a clock (for example a combinational logic with no register output) the `FREQ_HZ` property needs to be correctly set before validating the design.

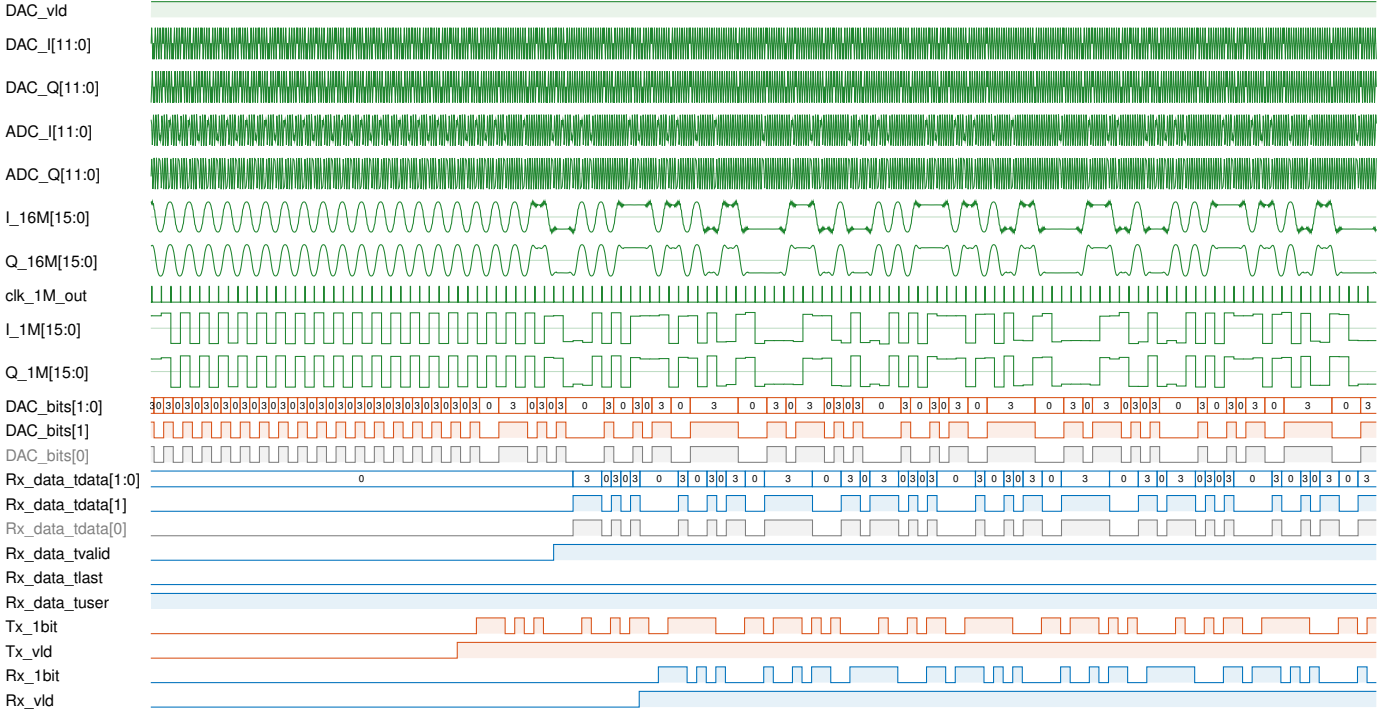
**Testbenches for block diagrams.** It is relatively difficult to simulate block diagrams than Verilog modules. The possible way is to generate the output products and find the correct module (name containing `impl`). Be careful when adding sources for simulation, and Tcl scripts are provided in [3] to ensure the correctness. Vivado can be buggy when updating sources from the block diagram (for both simulation and implementation), and therefore it is advised to double-check the netlist file timestamp.

## APPENDIX B FIGURES IN THIS PAPER

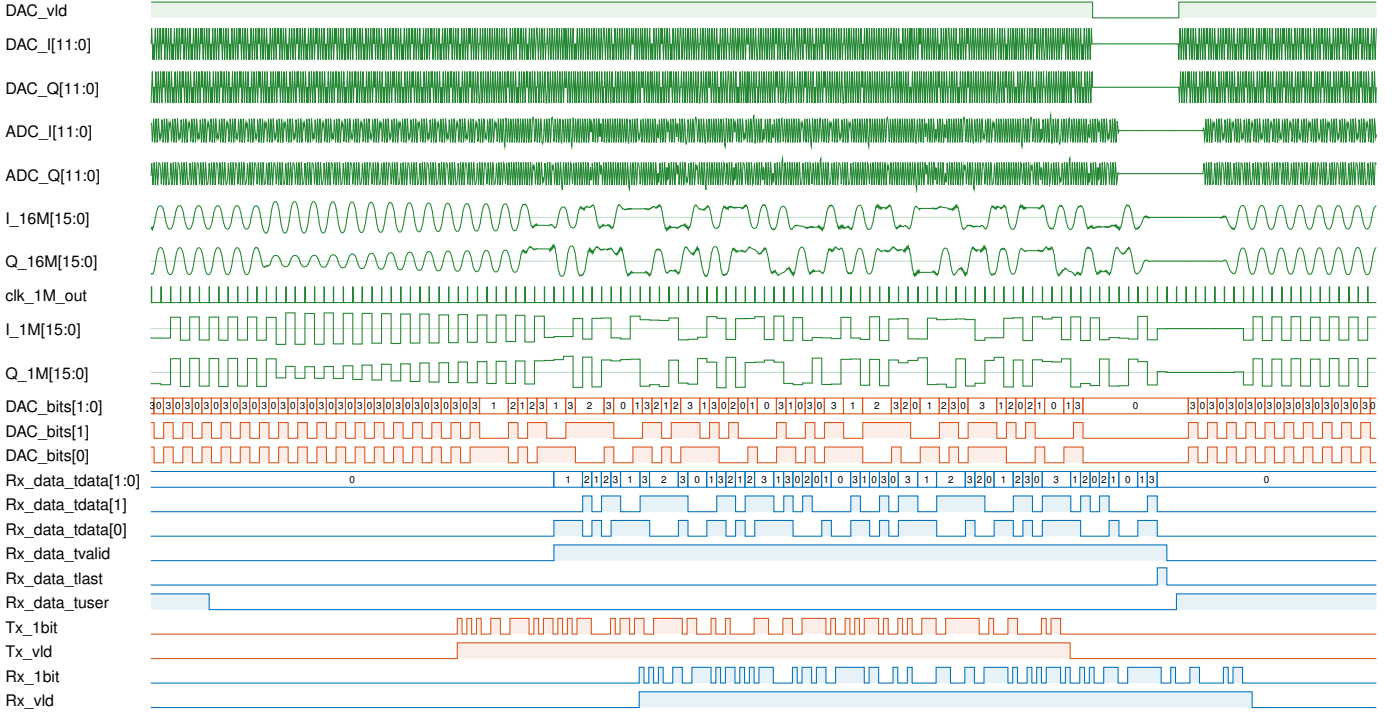
All figures except for block diagrams in this paper are created using TikZ, part of L<sup>A</sup>T<sub>E</sub>X. The way I create them is quite interesting, and you can find the source code in the GitHub repository [3].

## REFERENCES

- [1] R. Zhao, T. Woodford, T. Wei, K. Qian, and X. Zhang, "M-cube: A millimeter-wave massive MIMO software radio," in *Proc. ACM 26th Annu. Int. Conf. Mobile Comput. Network. (MobiCom)*, Sep. 2020, pp. 1–14.
- [2] W. Zhao, C. Li, Z. Ji, Z. Guo, X. Chen, Y. You, Y. Huang, X. You, and C. Zhang, "Flexible high-level synthesis library for linear transformations," *IEEE Trans. Circuits Syst. II*, 2023, to be published.
- [3] W. Zhao, "sdr-psk-fpga," GitHub repository, 2024. [Online]. Available: <https://github.com/Teddy-van-Jerry/sdr-psk-fpga>
- [4] Wuhan Labtech, "eNodeX 30B SDR innovation & implementation platform," 2024. [Online]. Available: <http://www.labtech.cn/Product-software-eNodeX-30B.html>
- [5] AMD, "Processor system reset module v5.0 product guide (PG164)," Nov. 2015. [Online]. Available: <https://docs.xilinx.com/v/u/en-US/pg164-proc-sys-reset>
- [6] —, "System integrated logic analyzer v1.1 product guide (PG261)," Feb. 2021. [Online]. Available: <https://docs.xilinx.com/v/u/en-US/pg261-system-ila>
- [7] —, "DDS compiler v6.0 product guide (PG141)," Jan. 2021. [Online]. Available: <https://docs.xilinx.com/v/u/en-US/pg141-dds-compiler>
- [8] F. James, "A review of pseudorandom number generators," *Comput. Phys. Commun.*, vol. 60, no. 3, pp. 329–344, Oct. 1990.
- [9] M. Simon and W. Lindsey, "Optimum performance of suppressed carrier receivers with Costas loop tracking," *IEEE Trans. Commun.*, vol. 25, no. 2, pp. 215–227, Feb. 1977.
- [10] F. Gardner, "A BPSK/QPSK timing-error detector for sampled receivers," *IEEE Trans. Commun.*, vol. 34, no. 5, pp. 423–429, May 1986.
- [11] AMD, "AXI external peripheral controller (EPC) v2.0 product guide (PG127)," Oct. 2016. [Online]. Available: <https://docs.xilinx.com/v/u/en-US/pg127-axi-epc>
- [12] W. Zhao, Y. You, L. Zhang, X. You, and C. Zhang, "OMPL-SBL algorithm for intelligent reflecting surface-aided mmWave channel estimation," *IEEE Trans. Veh. Technol.*, vol. 72, no. 11, pp. 15 121–15 126, Nov. 2023.
- [13] Y. You, W. Zhao, L. Zhang, X. You, and C. Zhang, "Beam pattern and reflection pattern design for channel estimation in RIS-assisted mmWave MIMO systems," *IEEE Trans. Veh. Technol.*, 2023, to be published, doi: [10.1109/TVT.2023.3309950](https://doi.org/10.1109/TVT.2023.3309950).
- [14] W. Zhao, C. Li, Z. Ji, Y. You, X. You, and C. Zhang, "Automatic timing-driven top-level hardware design for digital signal processing," in *Proc. IEEE 15th Int. Conf. ASIC (ASICON)*, Oct. 2023.
- [15] AMD, "Multiplier v12.0 product guide (PG108)," Nov. 2015. [Online]. Available: <https://docs.xilinx.com/v/u/en-US/pg108-mult-gen>



(a) A BPSK packet.



(b) A QPSK packet.

Fig. 10. System ILA results (some signals not shown). The system ILA has a window of 4,096, at the clock of 32.768 MHz (twice the sampling rate).

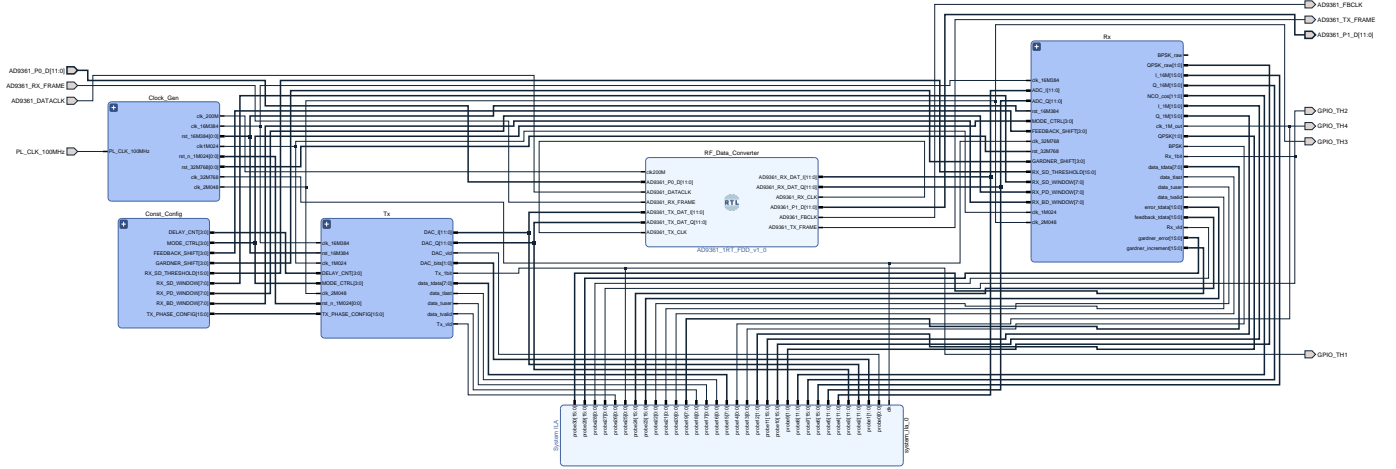


Fig. 11. Top block diagram.

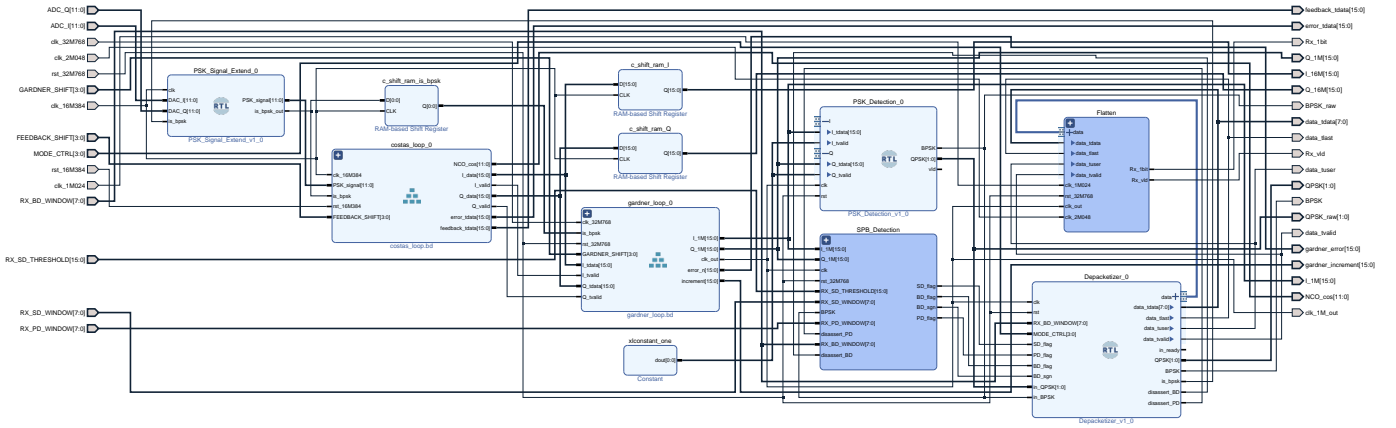


Fig. 12. Rx processor block diagram.

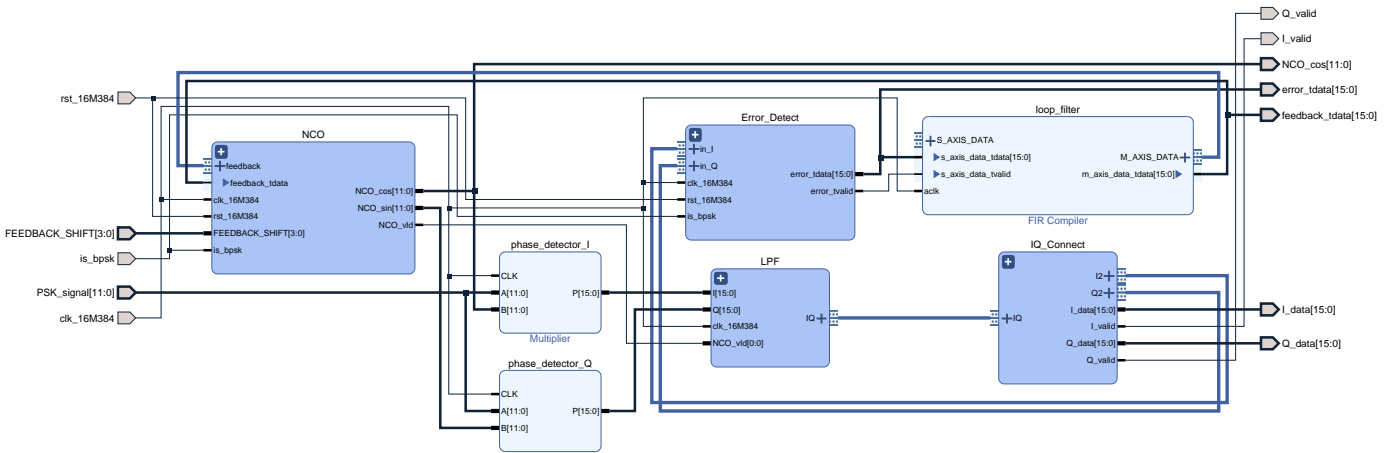


Fig. 13. Costas loop block diagram for carrier synchronization.